minerals

MDPI

Article

Geochemical Distribution, Integrated Contamination, and Human Health Risks of Potentially Toxic Elements in Najran Agricultural Soils, Saudi Arabia

Abdelbaset S. El-Sorogy * and Abdullah Al Shaiban

Geology and Geophysics Department, College of Science, King Saud University, Riyadh 11451, Saudi Arabia; 446910198@student.ksu.edu.sa

* Correspondence: asmohamed@ksu.edu.sa

Abstract

This study investigates the geochemical distribution, integrated contamination status, and human health risks of potentially toxic elements (PTEs) in 31 agricultural topsoil samples collected from Najran, southwestern Saudi Arabia. As, Co, Cr, Cu, Ni, Pb, and Zn were measured and interpreted using spatial distribution maps, the pollution load index (PLI), Nemerow integrated pollution index (PN), chronic daily intake (CDI), hazard quotient (HQ), hazard index (HI), cancer risk (CR), and lifetime cancer risk (LCR) for both children and adults. The measured concentrations (mg/kg) varied from 2–8 for As, 2–14 for Co, 11–50 for Cr, 5–50 for Cu, 9–50 for Ni, 2–28 for Pb, and 10–249 for Zn. Based on mean values (mg/kg), the PTEs followed the descending sequence Zn (52.94) > Cr (26.68) > Ni (24.55) > Cu (16.68) > Co (6.81) > Pb (6.65) > As (4.45). PLI values ranged between 0.117 and 0.642, with an average of 0.355, suggesting generally low combined pollution by multiple elements across all sampling locations. However, PN values extended from 0.137 to 1.930, classifying 27 locations as safe, 2 as warning-level sites, and 2 as slightly polluted, mainly due to elevated Zn and Pb levels. The assessment of non-carcinogenic risk indicated no exceedance of the level of concern, as total HI values ranged from 0.156 to 0.678 for children and from 0.017 to 0.075 for adults. On average, children had HI values about 9.1 times higher than adults, with soil ingestion representing the principal exposure route. The element-specific mean HI results indicated that As and Cr were the dominant contributors to non-carcinogenic risk. Carcinogenic risk was assessed for As, Cr, and Pb. Total LCR values ranged from 1.005×10^{-5} to 4.387×10^{-5} for children and from 4.460×10^{-6} to 1.950×10^{-5} for adults, remaining within the widely accepted or tolerable risk range. Among the carcinogenic elements, Cr accounted for the highest proportion of total LCR, contributing 68.67%–69.66%, followed by As with 30.09%–31.07%, while Pb made a very small contribution of only 0.25%–0.26%. In spatial terms, the greatest HI and LCR values were concentrated mainly in the western to central-western agricultural areas, where several elements relevant to health risk were present together.

Keywords: agricultural topsoils; potentially toxic elements; human health risk assessment; hazard index; lifetime cancer risk; Najran

Check for updates

Academic Editors: Yinxian Song, Yubo Wen and Saglara S. Mandzhieva

Received: 8 June 2026
Revised: 26 June 2026
Accepted: 29 June 2026
Published: 30 June 2026

Copyright: © 2026 by the authors. Licensee MDPI, Basel, Switzerland. This article is an open access article distributed under the terms and conditions of the Creative Commons Attribution (CC BY) license.

1. Introduction

Agricultural soils represent an important connection point among geological processes, crop production, ecosystem performance, and human well-being. They provide

the medium for plant growth, control the movement and availability of nutrients and water, and can serve either as long-term reservoirs or pathways for contaminants that may eventually reach plants, livestock, and people. Among the different types of soil pollutants, PTEs, such as As, Co, Cr, Cu, Ni, Pb, and Zn, are especially important because they persist in the environment, do not biodegrade, and can build up in surface soils over extended periods. Their occurrence in agricultural soils may originate from natural sources, including weathering of parent materials, mineralized rock units, inherited alluvial sediments, and wind-blown dust. However, their levels can also be elevated by human activities such as mining, industrial emissions, irrigation with wastewater, traffic-derived particles, application of manure, pesticide use, and phosphate fertilization [1]. The European Union-scale assessment of agricultural soils highlighted the importance of broad monitoring programs for As, Cd, Cr, Cu, Hg, Pb, Zn, Co, and Ni to protect food safety and guide soil-quality management [2].

People may be exposed directly to PTEs in agricultural soils through accidental ingestion of soil, skin contact, and inhalation of resuspended dust particles, or indirectly through the soil–plant–food pathway [3–5]. Some elements, including Cu, Co, Ni, and Zn, are essential for biological functions in small amounts, but they can become harmful when their concentrations exceed safe limits. In contrast, As and Pb are of major toxicological concern even at low exposure levels because they have no known essential biological function and may contribute to neurological, kidney, cardiovascular, developmental, and carcinogenic effects [6–8]. Research on agricultural soils and soil-crop systems has consistently indicated that health risk is controlled not only by the total concentration of elements in soil, but also by the exposure route, receptor category, element toxicity, mobility, and transfer into edible plant tissues [9,10]. Children are usually considered the more sensitive population group because they have lower body weight, higher soil ingestion relative to body mass, and more frequent hand-to-mouth activity [11,12].

Recent international research has progressively shifted from simply reporting element concentrations toward more integrated assessment approaches that combine spatial mapping, pollution indices, exposure estimation, and health-risk calculations for specific receptor groups [13]. Gong et al. [14] applied ecological and human-health risk models to agricultural soils in southwest China and highlighted the importance of assessing ingestion, dermal contact, and inhalation as separate exposure pathways. Spatial distribution analysis is important for connecting PTE enrichment patterns with ecological and human-health risks in agricultural soils [15]. In addition, recent multi-receptor and probabilistic investigations have shown that deterministic estimates may not adequately represent exposure uncertainty, and that children can remain the most vulnerable receptor group even when average risk levels appear to be acceptable [16,17].

In arid and semi-arid environments, assessing PTEs in agricultural soils is particularly complex because several natural and human-related factors may act together, including local geochemical background, atmospheric dust input, strong evaporation, irrigation management, weak leaching, and the use of farm amendments. This situation is highly relevant to Saudi Arabia, where agricultural areas are often developed on alluvial plains, wadi deposits, and sediments originating from varied geological source rocks [18–20]. Recent studies from Saudi Arabia (e.g., Al-Ahsa Oasis, Makkah, Al Lith) indicate that agricultural soils may generally exhibit low to moderate contamination levels, influenced by both geological factors and localized human activities. Children had higher estimated health risks than adults. influenced by both geological factors and localized human activities [21–23]. These findings establish an important regional reference, but they also emphasize that agricultural soils in arid settings need location-specific evaluation rather than broad regional assumptions.

Although interest in agricultural-soil health risk assessment has grown both globally and within Saudi Arabia, Najran in southwestern Saudi Arabia remains insufficiently studied from a human-health perspective. However, a detailed human-health risk assessment using sample-specific CDI, HQ, HI, CR, and LCR has not yet been comprehensively established. This study aims to fill this gap by examining seven contaminants of potential concern, namely As, Co, Cr, Cu, Ni, Pb, and Zn, and by integrating concentration data with spatial distribution mapping, the pollution load index (PLI), Nemerow integrated pollution index (P_N), and receptor-specific health-risk calculations. The main objectives are to: (i) assess the concentrations and spatial patterns of PTEs in agricultural soils from Najran; (ii) determine the overall contamination burden using PLI and P_N; (iii) estimate sample-based CDI, HQ, and HI for children and adults through ingestion, dermal contact, and inhalation pathways; (iv) quantify CR and LCR for As, Cr, and Pb; and (v) identify the key elements, exposure routes, receptor categories, and farm sites that contribute most to possible health concerns. The novelty of this study is its transition from interpreting Najran agricultural soils mainly through geochemical and ecological-risk indicators toward a spatially explicit human-health risk framework that can be directly compared with recent regional and international HHRA studies of agricultural soils.

2. Materials and Methods

2.1. Study Area, Sampling, and Analytical Methods

This study was structured as a screening-level assessment of human health risks related to PTEs in agricultural soils from Najran, southwestern Saudi Arabia. A total of 31 agricultural topsoil samples were collected in January 2026 from the 0–15 cm depth interval across cultivated farms in the Najran region (Figure 1). This sampling depth was chosen because it represents the near-surface soil horizon most influenced by farming activities, fertilizer application, irrigation, atmospheric dust deposition, and regular human contact. The positions of the sampling sites were recorded using GPS. Although the initial analytical work covered a wider group of elements, the present health-risk evaluation was restricted to As, Co, Cr, Cu, Ni, Pb, and Zn.

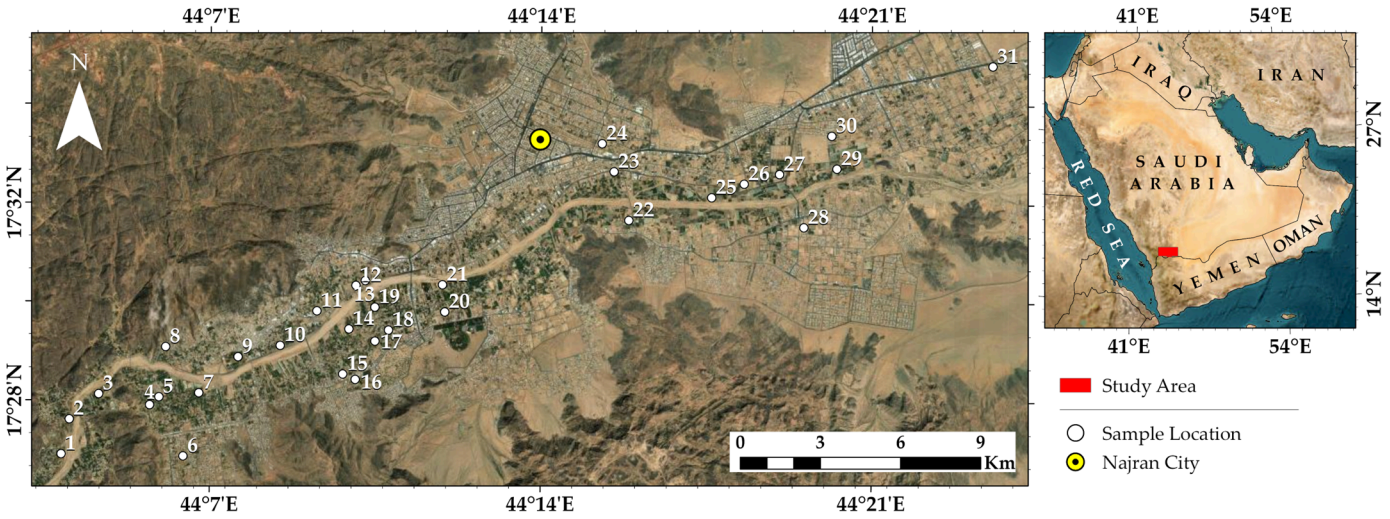

Figure 1. Location map of the Najran agricultural soil sampling sites; southwestern Saudi Arabia.

The collected soil samples were air-dried at room temperature, gently disaggregated, homogenized, and prepared for laboratory analysis. The samples were analyzed by ALS Arabia, Jeddah, Saudi Arabia. According to the ALS analytical certificate, sample preparation included pulverization using method PUL-31, in which up to 250 g of sample material was pulverized to 85% passing <75 µm. Multi-element analysis was performed using ALS

method ME-ICP41, which involves aqua regia digestion followed by Inductively Coupled Plasma-Atomic Emission Spectrometry (ICP-AES) determination for 36 elements. For the elements retained in the present assessment, the reported detection limits were 2 mg/kg for As, Pb, and Zn, and 1 mg/kg for Co, Cr, Cu, and Ni.

Analytical quality assurance and quality control were evaluated using the quality-control standards EMOG-17, GBM321-8, MRCA-21, and OREAS-45h, as reported in the ALS QC Certificate JD26028672 [24], together with reagent blanks and duplicate analyses. The standard results were within the target ranges reported by ALS, the blanks were below or equal to the corresponding detection limits, and duplicate analyses were within the laboratory target ranges. These QA/QC results support the reliability of the PTE concentrations used in the contamination and human-health risk calculations.

2.2. Integrated Contamination Indicators

The integrated contamination evaluation was conducted using the PLI, first proposed by Tomlinson et al. [25], together with the P_N, to assess the overall contamination pressure of the studied PTEs across the agricultural farms. The P_N is commonly applied as a comprehensive pollution indicator in soil-quality assessments [26]. The PLI produces a single site-specific value for total multi-element contamination by calculating the geometric mean of contamination factors. In comparison, the P_N combines the average contamination status with the highest element-specific contamination factor at each site. As a result, P_N is more responsive to isolated enrichment hotspots than PLI, particularly in soils with strong spatial heterogeneity [14,15].

For each element, the contamination factor was calculated as:

$$CF_i = \frac{C_i}{B_i}$$

The pollution load index was calculated as:

$$PLI = (CF_1 \times CF_2 \times CF_3 \times \cdots \times CF_n)^{1/n}$$

The Nemerow integrated pollution index was calculated as:

$$P_N = \sqrt{\frac{CF_{\max}^2 + CF_{\text{ave}}^2}{2}}$$

where CF_i represents the contamination factor for element i, C_i denotes the measured soil concentration of that element, and Bi refers to its corresponding background concentration. The term n indicates the number of elements included in the assessment. CF_{max} is the highest contamination factor recorded among the selected elements at a specific sampling location, while CF_{ave} represents the mean contamination factor for that same location.

2.3. Human Health Risk Assessment

Human health risk was evaluated using CDI, HQ, HI, CR, and LCR. These indicators are commonly used in health-risk assessments of agricultural soils and were applied in this study to allow comparison with recent regional and international research [13,23,27]. Risk calculations were performed separately for children and adults. Incidental soil ingestion, dermal contact with soil, and inhalation of resuspended soil particles were included as three exposure routes.

Pb was included in the HQ/HI and CR/LCR calculations to maintain comparability with recent agricultural-soil HHRA studies that evaluate Pb alongside other PTEs [16,28]; however, Pb-related outputs are interpreted only as comparative screening estimates, not

as regulatory blood-lead-based risks, because the U.S. EPA treats lead as a special case within the standard RSL framework [29]. Similarly, Cr-related cancer-risk estimates were based on total Cr rather than Cr(VI) and should therefore be regarded as screening-level comparative values rather than speciation-specific carcinogenic risk estimates [30].

For soil ingestion, chronic daily intake was calculated as:

$$CDI_{ing} = \frac{C \times IngR \times EF \times ED \times CF}{BW \times AT}$$

For inhalation of resuspended soil particles, chronic daily intake was calculated as:

$$CDI_{inh} = \frac{C \times InhR \times EF \times ED}{PEF \times BW \times AT}$$

For dermal contact with soil, chronic daily intake was calculated as:

$$CDI_{derm} = \frac{C \times SA \times AF \times ABS \times EF \times ED \times CF}{BW \times AT}$$

The pathway-specific hazard quotient was calculated as:

$$HQ = \frac{CDI}{RfD}$$

The cumulative non-carcinogenic hazard index was calculated as:

$$HI = \sum HQ = HQ_{ing} + HQ_{derm} + HQ_{inh}$$

Carcinogenic risk was calculated for As, Cr, and Pb using the available cancer slope factors. The pathway-specific cancer risk was calculated as:

$$CR = CDI \times CSF$$

The total lifetime cancer risk was calculated as:

$$LCR = \sum CR = CR_{ing} + CR_{derm} + CR_{inh}$$

where C represents the soil concentration of the element (mg/kg). However, Table 1 presents the exposure parameters used for estimating chronic daily intake and health risk of PTEs in Najran soil [31,32]. HQ or HI values below 1 were considered to indicate that non-carcinogenic adverse effects are unlikely under the exposure assumptions applied in this study. In contrast, values exceeding 1 were taken to suggest a possible non-carcinogenic health concern [23,33,34]. For carcinogenic risk, LCR values below 1×10^{-6} were classified as negligible, values from 1×10^{-6} to 1×10^{-4} were regarded as acceptable or tolerable, and values above 1×10^{-4} were interpreted as indicating potential carcinogenic concern. This interpretation follows the classification commonly adopted in agricultural-soil health-risk assessments [13,35]. The toxicity parameters applied in the risk calculations, including pathway-specific RfDs, dermal absorption factors, and cancer slope factors, are presented in Table 2.

The HHRA applied in this study should be interpreted as a direct soil-exposure screening assessment. It evaluates incidental ingestion of soil, dermal contact, and inhalation of resuspended soil particles, but it does not quantify dietary exposure through crop consumption. Therefore, the calculated CDI, HQ, HI, CR, and LCR values indicate potential risk from soil-contact pathways rather than total agricultural food-chain exposure.

Table 1. Exposure parameters used for estimating CDI and HI of PTEs in Najran soil.

Parameter	Symbol	Unit	Child	Adult
Soil ingestion rate	IngR	mg/day	2.00×10^{2}	1.00×10^{2}
Inhalation rate	InhR	m^3/day	7.60×10^{0}	2.00×10^{1}
Exposure frequency	EF	days/year	3.50×10^{2}	3.50×10^{2}
Exposure duration	ED	year	6.00×10^{0}	2.40×10^{1}
Body weight	BW	kg	1.50×10^{1}	7.00×10^{1}
Average time for non-carcinogenic risk	ATnc	days	2.19×10^{3}	8.76×10^{3}
Average time for carcinogenic risk	ATc	days	2.56×10^{4}	2.56×10^{4}
Particulate emission factor	PEF	m^3/kg	1.36×10^{9}	1.36×10^{9}
Skin surface area	SA	cm^2	2.80×10^{3}	5.70×10^{3}
Adherence factor	AF	mg/cm^2	2.00×10^{-1}	7.00×10^{-2}
Dermal absorption factor	ABS	unitless	1.00×10^{-3}	1.00×10^{-3}
Conversion factor	CF	kg/mg	1.00×10^{-6}	1.00×10^{-6}

Table 2. Toxicity parameters used for non-carcinogenic and carcinogenic risk assessment of PTEs in Najran soil.

PTEs	Oral RfD	Dermal RfD	Inhalation RfD	RfD Unit	CSF_{ing}	CSF_{derm}	CSF_{inh}
As	3.00×10^{-4}	1.23×10^{-4}	3.00×10^{-4}	mg/kg/day	1.50×10^{0}	3.66×10^{0}	1.51×10^{1}
Co	2.00×10^{-2}	1.60×10^{-2}	—	mg/kg/day	—	—	—
Cr	3.00×10^{-3}	6.00×10^{-5}	2.86×10^{-5}	mg/kg/day	5.00×10^{-1}	2.00×10^{1}	4.20×10^{1}
Cu	4.00×10^{-2}	4.02×10^{-2}	1.20×10^{-2}	mg/kg/day	—	—	—
Ni	2.00×10^{-2}	5.40×10^{-3}	2.06×10^{-2}	mg/kg/day	—	—	—
Pb	3.50×10^{-3}	3.25×10^{-4}	3.52×10^{-3}	mg/kg/day	8.50×10^{-3}	—	4.20×10^{-2}
Zn	3.00×10^{-1}	6.00×10^{-2}	3.00×10^{-1}	mg/kg/day	—	—	—

2.4. Statistical and Spatial Analysis

Descriptive statistical measures, including the minimum, maximum, mean, and standard deviation, were applied to summarize PTE concentrations as well as the derived contamination and health-risk indices. Values of PLI, P_N, CDI, HQ, HI, CR, and LCR were calculated individually for all 31 sampling locations. The site-specific outputs were then connected with their corresponding geographic coordinates and mapped within a GIS platform to examine spatial trends, contamination intensity, and potential health-risk hotspots across the cultivated farms. This spatial procedure is consistent with recent agricultural-soil investigations that combine GIS tools, contamination indices, and HHRA methods to detect localized risk patterns instead of depending solely on broad average values.

3. Results and Discussion

3.1. Concentration Levels and Spatial Distribution of Selected PTEs

PTE concentrations (mg/kg) in Najran agricultural soils varied from 2 to 8 (As), 2 to 14 (Co), 11 to 50 (Cr), 5 to 50 (Cu), 9 to 50 (Ni), 2 to 28 (Pb), and 10 to 249 (Zn) (Table S1). On the basis of mean concentrations, the elements decreased in the sequence Zn > Cr >

Ni > Cu > Co > Pb > As (Table 3). The greatest relative variation was recorded for Zn, followed by Pb and Cu, suggesting that these elements are more influenced by localized enrichment processes than by a consistent regional background pattern. This observation is also supported by the boxplots in Figure 2, where Zn exhibits the broadest spread and a clear outlier at sample 2, whereas Pb shows a notable outlier at sample 16. Comparable heterogeneous spatial patterns of PTEs in agricultural soils have been documented in areas where field-scale soil management, parent materials, and sediment redistribution processes interact [15].

Table 3. Descriptive statistics of PTEs (mg/kg) in Najran soils.

PTEs	Minimum	Maximum	Mean	SD
As	2.00	8.00	4.45	1.88
Co	2.00	14.00	6.81	2.89
Cr	11.00	50.00	26.68	9.38
Cu	5.00	50.00	16.68	8.97
Ni	9.00	50.00	24.55	10.65
Pb	2.00	28.00	6.65	4.87
Zn	10.00	249.00	52.94	40.44

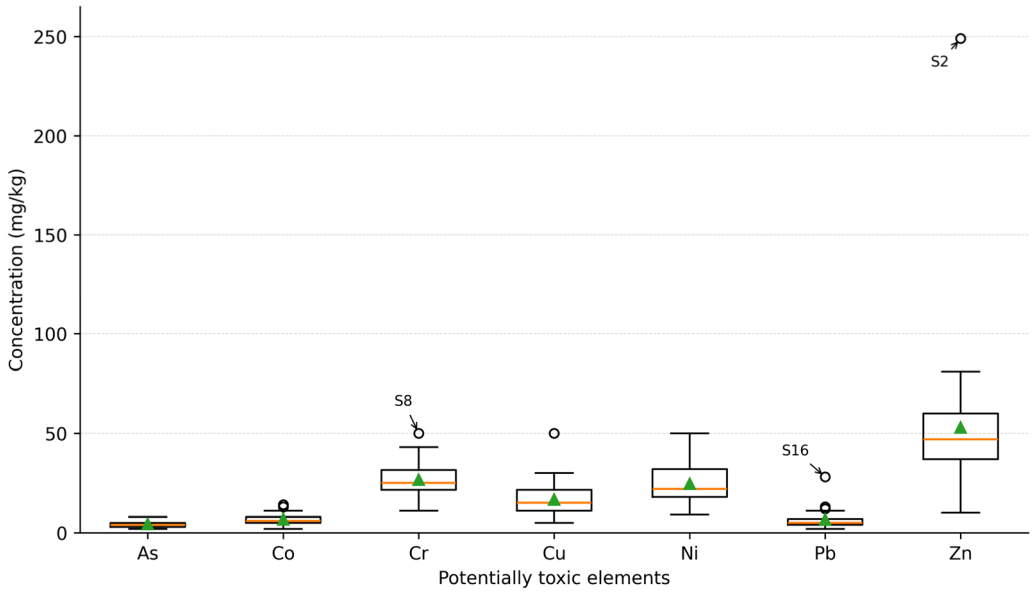

Figure 2. Boxplots of PTE concentrations; boxes, lines, green triangles, and circles indicate interquartile ranges, medians, means, and outliers, respectively.

The interpolated spatial maps (Figure 3) indicate that Co, Cr, and Ni display generally similar distribution patterns. Their concentrations are relatively higher in the western to central-western part of the cultivated farms, whereas lower levels occur mainly toward the eastern and north-eastern areas. This spatial trend agrees with the sample-specific maximum values observed at sample 8, where Co, Cr, and Ni reached 14, 50, and 50 mg/kg, respectively. The same western to central-western sector also includes several farms with comparatively high multi-element signatures, while sample 23 represents one of the lowest-concentration locations for these elements. The consistent association among Co, Cr, and Ni indicates that their spatial distribution is probably governed mainly by inherited lithogenic or alluvial contributions rather than by a single local anthropogenic source [14,36].

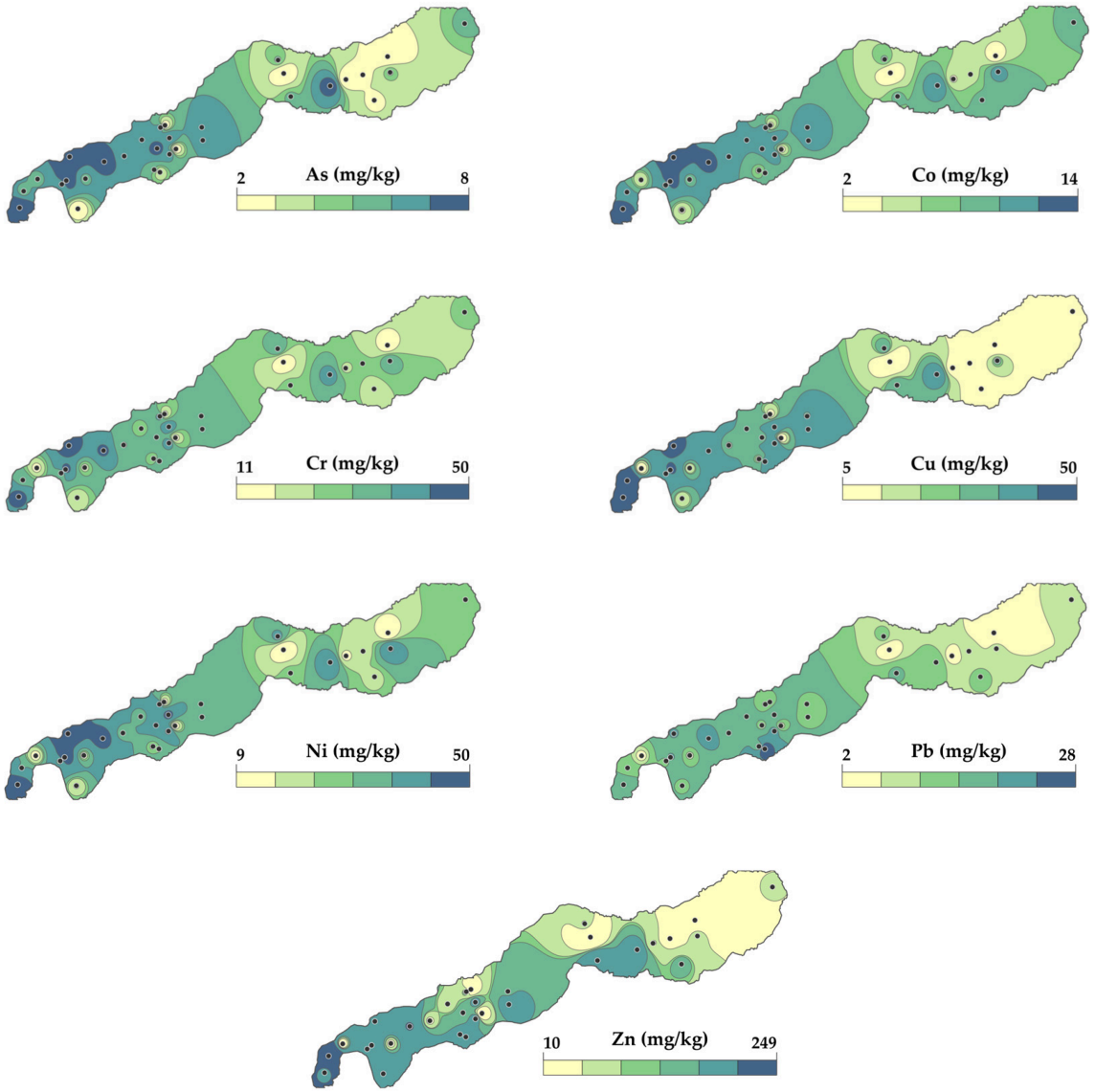

Figure 3. Interpolated spatial distribution of the PTEs in Najran agricultural topsoils.

Arsenic shows a generally similar but less continuous spatial distribution. The highest As concentrations were recorded at samples 1, 5, and 8 (8 mg/kg), while the lowest concentrations occurred at samples 6, 13, 18, 23, 26, and 30 (Table S1). In spatial terms, As is moderately enriched in some western and central-western farm areas, although its pattern is more irregular than those observed for Co, Cr, and Ni. This distribution suggests that As is partly associated with the western geochemical setting, but it may also be influenced by local differences in sediment texture, accumulation of fine particles, or farm-level inputs [9]. In contrast, Cu and Zn are characterized by a pronounced localized enrichment in the southwestern sector of the study area. The most prominent anomaly is observed at sample 2, where Cu and Zn concentrations reach 50 and 249 mg/kg, respectively, clearly exceeding the values measured in most nearby farms. This restricted spatial pattern suggests that the enrichment of Cu and Zn is not distributed across the whole region, but instead represents a farm-scale hotspot imposed on the general geochemical background. In agricultural soils, such Cu-Zn anomalies may result from repeated applications of fertilizers, manure, pesticides, or other farming amendments, although the composition of natural sediments may also play a role [37].

Lead shows a distribution pattern that differs from both the Co-Cr-Ni association and the localized Cu-Zn anomaly. The highest Pb concentration was measured at sample 16, where it reached 28 mg/kg, whereas most of the remaining samples showed considerably lower values. Accordingly, Pb forms a localized anomaly in the central part of the study area rather than showing a continuous west–east trend or matching the Cu-Zn enrichment observed at sample 2. This spatial separation indicates that Pb enrichment may be associated with a different local source or site-specific micro-environmental factor, such as localized dust accumulation, traffic-derived particulates, suspended materials introduced through irrigation, or small-scale variation in alluvial parent sediments [36,37].

3.2. Integrated Contamination Assessment

The computed PLI values varied between 0.117 and 0.642, with an average of 0.355 ± 0.139. Since all samples showed PLI values below 1 (Tables 4 and S2), the investigated agricultural soils can be classified as having low overall multi-element contamination. The maximum PLI was observed at sample 8, followed by samples 5, 9, and 1. These sites generally coincide with the western to central-western part of the study area, where several elements, particularly As, Co, Cr, Cu, and Ni, occurred at comparatively higher concentrations. By contrast, sample 23 recorded the lowest PLI value, reflecting its generally low concentrations of most of the selected PTEs. This type of PLI-based assessment is widely applied to describe cumulative contamination pressure from multiple elements and to separate broad pollution conditions from isolated single-element enrichment patterns [27,37].

Table 4. Summary statistics and classification of the PLI and PN in Najran agricultural topsoils.

Index	Minimum	Maximum	Mean	SD	Dominant Class
PLI	0.117	0.642	0.355	0.139	Low/no overall pollution
PN	0.137	1.930	0.500	0.326	Safe

The PN values exhibited a broader range than the PLI values, extending from 0.137 to 1.930, with a mean of 0.500 ± 0.326. The majority of the samples (27 out of 31) were categorized as safe class. Samples 5 and 9 were assigned to the warning category, while samples 2 and 16 were classified as slightly polluted (Table S2). The contrast between the PLI and PN classifications highlights the greater sensitivity of PN to individual element anomalies, since its calculation incorporates the highest contamination factor at each site. Similar applications of Nemerow-type integrated indices in recent agricultural-soil studies have been used to detect localized heavy-metal pressure and to separate warning or slightly polluted sites from areas that are generally safe [38,39].

The two samples assigned to the slight-pollution category by PN were influenced by different dominant elements. For sample 2, the increased PN value (Figure 4) was mainly controlled by the high Zn contamination factor, which corresponds to the pronounced Zn hotspot shown in the spatial distribution map (Figure 3). In contrast, the PN value at sample 16 was largely related to elevated Pb, consistent with the central Pb anomaly. This difference shows that PN does not merely reflect the broader regional spatial pattern, but instead emphasizes localized element-specific anomalies at individual sampling sites. Similar localized enrichments of Zn and Pb have been documented in agricultural soils influenced by both geogenic and anthropogenic factors, especially where local inputs overlap with variable parent materials or mineralized geological backgrounds [14,15,37].

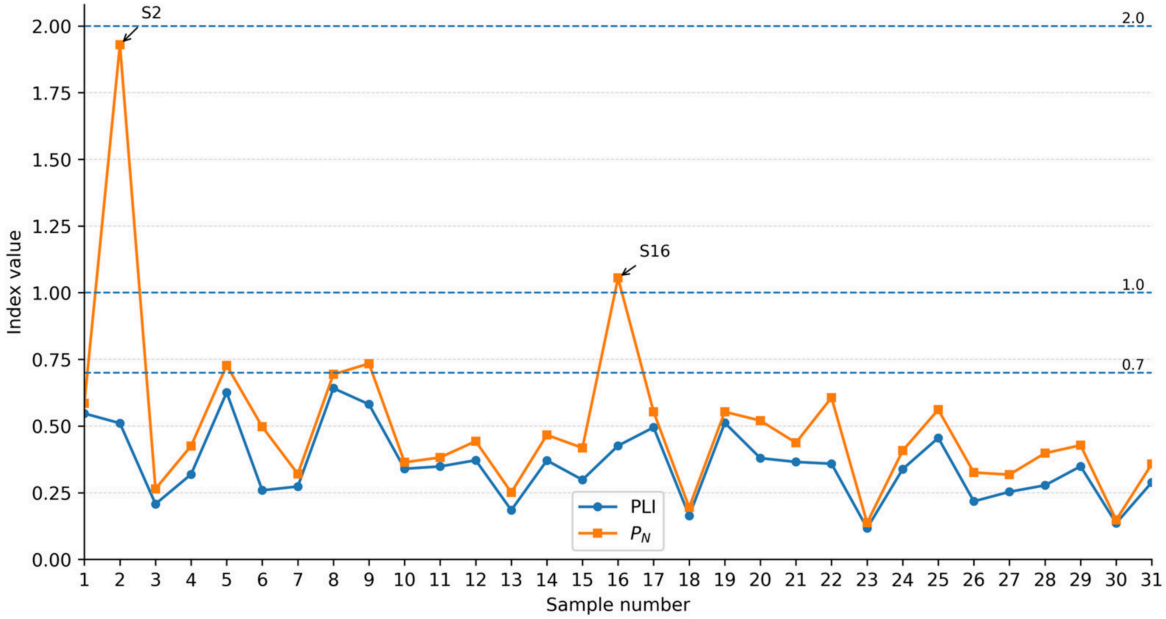

Figure 4. Site-specific values of the PLI and PN for Najran agricultural topsoils.

3.3. Non-Carcinogenic Human Health Risk

The results of CDI, pathway-specific HQ, and element-specific HI show that non-carcinogenic risk stayed below the level of concern for both children and adults. For children, the cumulative HI varied from 0.156 to 0.678, with an average of 0.374 ± 0.141. For adults, HI values ranged from 0.017 to 0.075, with a mean of 0.041 ± 0.015 (Table 5). Since all HI values were below 1, harmful non-carcinogenic effects are not expected under the screening-level exposure assumptions used in this study. However, children consistently recorded higher risk values than adults, with the mean HI for children being about 9.1 times greater than that for adults. This difference between receptor groups is mainly related to children's lower body weight, greater soil intake relative to body mass, and age-specific exposure behaviours [40–43].

The pathway-specific results indicate that incidental soil ingestion was by far the dominant route for non-carcinogenic exposure. For children, the mean HQing values were substantially higher than the corresponding dermal and inhalation values for every element (Table 5). A similar pattern was found for adults, although the absolute values were considerably lower. The inhalation pathway made a negligible contribution to total HI because its calculated intake is greatly reduced by the particle emission factor. Dermal contact also represented only a minor share of the total risk compared with ingestion [21,44].

At the elemental scale, the average total HI values for children decreased in the following order (Table S3): As (0.191) > Cr (0.130) > Pb (0.025) > Ni (0.016) > Cu (0.005) > Co (0.004) > Zn (0.002). The same sequence was observed for adults, with mean HI values of 0.021 (As), 0.015 (Cr), 0.003 (Pb), 0.002 (Ni), 0.0006 (Cu), 0.0005 (Co), and 0.0002 (Zn). These findings show that As and Cr were the main contributors to non-carcinogenic risk. By contrast, Zn made the smallest contribution to HI, even though it had the highest mean concentration in the soil. This demonstrates that non-carcinogenic risk is not governed only by soil concentration, but also by the relationship between estimated dose and pathway-specific reference values. Similar contrasts between elemental enrichment and hazard contribution have been reported in contaminated farmland soils and multi-receptor agricultural-soil assessments, where

Cr, As, Pb, or Ni may dominate health-risk estimates even when they are not the most abundant elements [16,41,45].

Table 5. Average CDI, HQ, and HI values for non-carcinogenic risk of PTEs for children and adults.

PTEs	Children						
	CDI_{ing}	CDI_{derm}	CDI_{inh}	HQ_{ing}	HQ_{derm}	HQ_{inh}	HI
As	5.69×10^{-5}	1.59×10^{-7}	1.59×10^{-9}	1.897×10^{-1}	1.296×10^{-3}	5.301×10^{-6}	1.910×10^{-1}
Co	8.70×10^{-5}	2.44×10^{-7}	2.43×10^{-9}	4.351×10^{-3}	1.523×10^{-5}	—	4.366×10^{-3}
Cr	3.41×10^{-4}	9.55×10^{-7}	9.53×10^{-9}	1.137×10^{-1}	1.592×10^{-2}	3.332×10^{-4}	1.299×10^{-1}
Cu	2.13×10^{-4}	5.97×10^{-7}	5.96×10^{-9}	5.331×10^{-3}	1.485×10^{-5}	4.965×10^{-7}	5.346×10^{-3}
Ni	3.14×10^{-4}	8.79×10^{-7}	8.77×10^{-9}	1.569×10^{-2}	1.627×10^{-4}	4.257×10^{-7}	1.586×10^{-2}
Pb	8.50×10^{-5}	2.38×10^{-7}	2.37×10^{-9}	2.427×10^{-2}	7.320×10^{-4}	6.744×10^{-7}	2.501×10^{-2}
Zn	6.77×10^{-4}	1.90×10^{-6}	1.89×10^{-8}	2.256×10^{-3}	3.158×10^{-5}	6.304×10^{-8}	2.288×10^{-3}
PTEs	**Adults**						
	CDI_{ing}	CDI_{derm}	CDI_{inh}	HQ_{ing}	HQ_{derm}	HQ_{inh}	HI
As	6.10×10^{-6}	2.43×10^{-8}	8.97×10^{-10}	2.033×10^{-2}	1.978×10^{-4}	2.989×10^{-6}	2.053×10^{-2}
Co	9.32×10^{-6}	3.72×10^{-8}	1.37×10^{-9}	4.662×10^{-4}	2.325×10^{-6}	—	4.685×10^{-4}
Cr	3.65×10^{-5}	1.46×10^{-7}	5.37×10^{-9}	1.218×10^{-2}	2.430×10^{-3}	1.879×10^{-4}	1.480×10^{-2}
Cu	2.28×10^{-5}	9.12×10^{-8}	3.36×10^{-9}	5.711×10^{-4}	2.268×10^{-6}	2.800×10^{-7}	5.737×10^{-4}
Ni	3.36×10^{-5}	1.34×10^{-7}	4.95×10^{-9}	1.681×10^{-3}	2.485×10^{-5}	2.401×10^{-7}	1.706×10^{-3}
Pb	9.10×10^{-6}	3.63×10^{-8}	1.34×10^{-9}	2.601×10^{-3}	1.118×10^{-4}	3.803×10^{-7}	2.713×10^{-3}
Zn	7.25×10^{-5}	2.89×10^{-7}	1.07×10^{-8}	2.417×10^{-4}	4.822×10^{-6}	3.555×10^{-8}	2.466×10^{-4}

The maximum element-specific HI values provide additional support for this conclusion. Among children, the highest maximum HI values were associated with As (0.343), Cr (0.244), and Pb (0.105), while Zn and Co remained low even at their peak concentrations. A similar pattern was observed for adults, where As, Cr, and Pb again showed the highest maximum values, reaching 0.037, 0.028, and 0.011, respectively. Thus, the strong Zn enrichment recorded at sample 2 does not correspond to the greatest non-carcinogenic health risk. Instead, elements with higher toxicological significance, especially As and Cr, had a stronger effect on HI values.

The total non-carcinogenic hazard index was below the threshold value of 1 at every sampling location for both children and adults (Figure 5). This confirms that significant non-carcinogenic effects are unlikely under the screening-level assumptions adopted in this study. Nevertheless, children showed consistently higher HI values than adults. The highest child HI values were observed at samples 8, 5, 1, 9, and 19, which are mainly situated in the western to central-western part of the cultivated area, where several PTEs, particularly As, Co, Cr, and Ni, displayed relatively elevated concentrations. The maximum HI was recorded at sample 8, with values of 0.678 for children and 0.075 for adults (Figure 5). This spatial distribution suggests that cumulative non-carcinogenic risk is mainly controlled by the combined presence of several moderately enriched elements rather than by a single-element anomaly, shown that presenting HI at the sampling-location scale is useful for recognizing local priority areas that may not be evident from summary statistics alone [46–48].

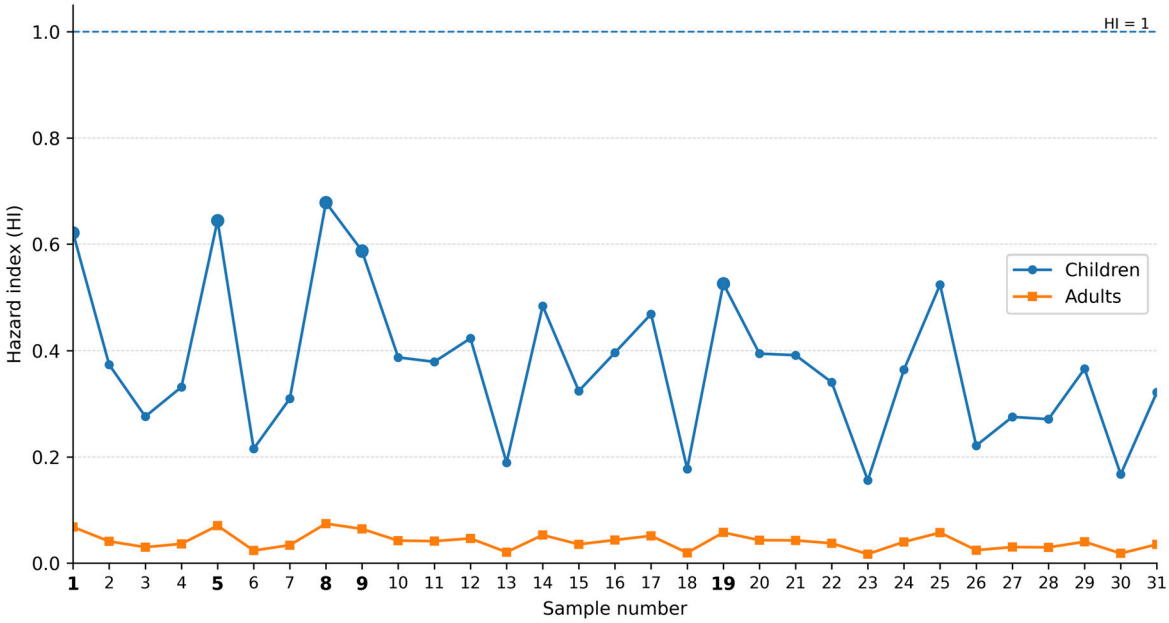

Figure 5. Site-specific non-carcinogenic HI values for children and adults in Najran soils. Bold sample numbers indicate the main child-HI hotspots.

3.4. Carcinogenic Human Health Risk

The calculated total LCR values for As, Cr, and Pb in children varied from 1.005×10^{-5} to 4.387×10^{-5}, with an average of $2.372 \times 10^{-5} \pm 8.586 \times 10^{-6}$. For adults, total LCR values ranged between 4.460×10^{-6} and 1.950×10^{-5}, with a mean of $1.054 \times 10^{-5} \pm 3.810 \times 10^{-6}$ (Table 6). Accordingly, all LCR values for both receptor groups were within the commonly accepted or tolerable interval of 1×10^{-6} to 1×10^{-4}, with no value exceeding 1×10^{-4} (Table S4). These results indicate that the carcinogenic risk associated with Najran agricultural soils remains within the tolerable range under the screening-level assumptions used in this study [16,28,30].

Table 6. Average CR and LCR values for As, Cr, and Pb for children and adults.

PTEs	Children			
	CR_{ing}	CR_{derm}	CR_{inh}	LCR
As	7.318×10^{-6}	4.999×10^{-8}	2.058×10^{-9}	7.370×10^{-6}
Cr	1.462×10^{-5}	1.637×10^{-6}	3.431×10^{-8}	1.629×10^{-5}
Pb	6.190×10^{-8}	—	8.546×10^{-12}	6.191×10^{-8}
PTEs	**Adults**			
	CR_{ing}	CR_{derm}	CR_{inh}	LCR
As	3.136×10^{-6}	3.053×10^{-8}	4.643×10^{-9}	3.171×10^{-6}
Cr	6.265×10^{-6}	9.999×10^{-7}	7.739×10^{-8}	7.342×10^{-6}
Pb	2.653×10^{-8}	—	1.928×10^{-11}	2.655×10^{-8}

At the elemental scale, Cr made the largest contribution to total carcinogenic risk, followed by As, while the contribution of Pb was very small. For children, the mean element-specific LCR values decreased in the order Cr (1.629×10^{-5}) > As (7.370×10^{-6}) > Pb (6.191×10^{-8}). A similar ranking was obtained for adults, with mean LCR values of 7.342×10^{-6} (Cr), 3.171×10^{-6} (As), and 2.655×10^{-8} (Pb). These results show that the carcinogenic-risk pattern was driven mainly by Cr and As rather than Pb, even though Pb

displayed localized enrichment at sample 16. The strong role of Cr in cancer-risk screening is consistent with recent agricultural-soil studies that identified Cr as a major contributor to overall carcinogenic risk [30,49,50]. The pathway-specific CR results show that ingestion represented the main carcinogenic exposure route for As, Cr, and Pb. For children, the mean CRing values were 1.462×10^{-5} (Cr), 7.318×10^{-6} (As), and 6.190×10^{-8} (Pb), whereas the dermal and inhalation pathways contributed much lower values. Adults followed the same exposure-route pattern, although their absolute CR values were lower. The dominance of ingestion is expected because this pathway is directly influenced by soil intake rate and contaminant concentration. In contrast, inhalation risk is strongly reduced by the particle emission factor [10,51].

As-related LCR values were consistently greater for children than for adults and generally remained within the 10^{-6}–10^{-4} risk range (Figure 6a). Among the three assessed elements, Cr generated the highest element-specific LCR values, confirming that it was the main driver of carcinogenic risk in the study area (Figure 6b). By comparison, Figure 6c indicates that Pb-related LCR values were substantially lower than those calculated for As and Cr at all sites, with most samples remaining close to or below 10^{-7}. Accordingly, the geochemically identified Pb hotspot does not represent a major contributor to carcinogenic risk within the adopted comparative assessment framework, showing that health-risk priority depends on both exposure dose and element-specific toxicity, rather than on concentration level alone [28,49,52].

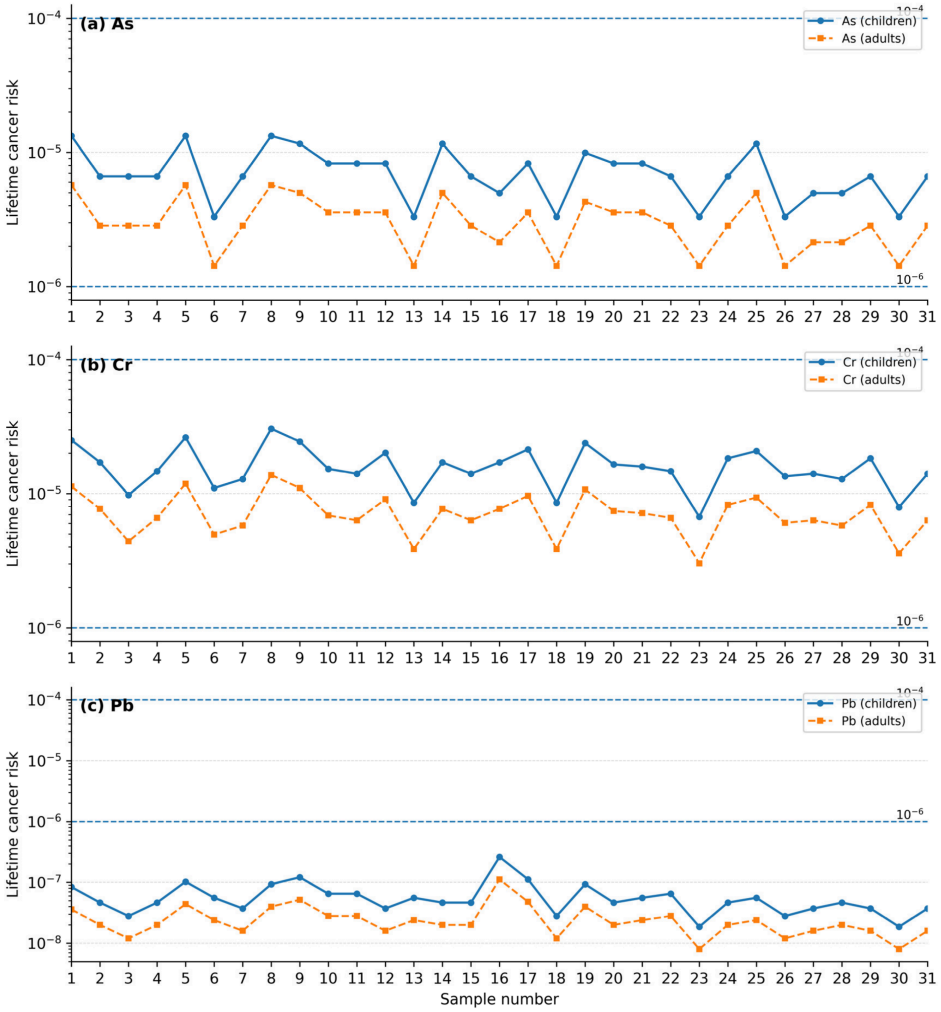

Figure 6. Site-specific element-specific LCR of (**a**) As, (**b**) Cr, and (**c**) Pb for children and adults in Najran soils.

Spatially, the greatest total LCR values were mainly observed at samples 8, 5, 1, 9, and 19 (Figure 6). These locations correspond to the same broad western to central-western sector where elevated non-carcinogenic HI values were also recorded. The highest total LCR occurred at sample 8, reaching 4.387×10^{-5} for children and 1.950×10^{-5} for adults. This distribution reflects the combined occurrence of relatively elevated As and Cr, along with other transition metals, rather than the influence of a single Pb anomaly. Therefore, cancer-risk prioritization in Najran soils should mainly target farms where As and Cr are jointly enriched [17,43,53,54].

3.5. Limitations

This study represents a screening-level assessment based on total soil concentrations and standard exposure assumptions. Because bioaccessible fractions were not measured, the calculated CDI, HQ, HI, CR, and LCR values may not fully represent the actual internal dose. In addition, crop tissues were not analyzed; therefore, the results describe direct soil-exposure risk rather than dietary exposure through the soil–plant–food pathway. Further uncertainty is related to the absence of soil physicochemical parameters, including pH, organic matter, redox conditions, texture, and particle-size distribution, which can strongly influence PTE mobility, bioavailability, and toxicity. Formal WRB soil classification was also not possible because full soil-profile descriptions and diagnostic horizons were not available. In addition, Cr-related cancer risk was estimated from total Cr rather than Cr(VI), while Pb-related values were retained only as comparative screening estimates rather than blood-lead-based regulatory risks. Finally, the interpolation maps are spatial approximations based on 31 samples and should not be interpreted as exact contamination boundaries.

4. Conclusions

This study presents a sample-based screening evaluation of integrated contamination and human health risks related to As, Co, Cr, Cu, Ni, Pb, and Zn in agricultural topsoils from Najran, southwestern Saudi Arabia. The findings indicate that the soils are not subject to extensive multi-element pollution, as all PLI values remained below 1. Nevertheless, the PN identified restricted site-level enrichment, especially the Zn anomaly at sample 2 and the Pb anomaly at sample 16. This confirms that localized hotspots may be overlooked when assessment relies only on general pollution indices or mean concentration values.

The health-risk evaluation showed that non-carcinogenic risk remained below the level of concern for both children and adults. Total HI values ranged from 0.156 to 0.678 for children and from 0.017 to 0.075 for adults. Children were consistently identified as the more vulnerable receptor group, with a mean HI approximately 9.1 times higher than that of adults. For all elements and both receptor groups, incidental soil ingestion was the main exposure route, while dermal contact and inhalation made substantially smaller contributions. Although Zn recorded the highest average concentration in the soils, its contribution to HI was very limited. In contrast, As and Cr were the dominant contributors to non-carcinogenic risk, confirming that health risk depends on toxicity-weighted exposure rather than concentration level alone.

Carcinogenic risk estimates for As, Cr, and Pb were within the commonly accepted or tolerable range. Total LCR values varied from 1.005×10^{-5} to 4.387×10^{-5} for children and from 4.460×10^{-6} to 1.950×10^{-5} for adults. Cr was the main contributor to total LCR, representing approximately 68.7%–69.7% of the total risk, followed by As (30.1%–31.1%). In contrast, Pb contributed less than 0.3%, despite its localized enrichment. The highest HI and LCR values were concentrated mainly in the western to central-western farms, particularly near sample 8, where several elements relevant to health risk occurred together.

Future investigations should extend this screening assessment by incorporating soil physicochemical properties, WRB-based soil classification, oral bioaccessibility, Cr speciation, Pb-specific modelling, and crop-transfer measurements to evaluate the complete soil–plant–human exposure pathway.

Supplementary Materials: The following supporting information can be downloaded at: https://www.mdpi.com/article/10.3390/min16070693/s1, Figure S1: Mean element-wise contribution of As, Cr, and Pb to total lifetime cancer risk (LCR) for children and adults in Najran agricultural topsoils; Table S1: Coordination and PTEs concentration (mg/kg) for Najran topsoil samples; Table S2: Site-specific PLI and PN values for the 31 Najran agricultural topsoil samples; Table S3: HI of selected PTEs for non-carcinogenic risk in adults and children in Najran agricultural topsoils; Table S4: Site-specific LCR values for As, Cr, and Pb in Najran agricultural topsoils for children and adults.

Author Contributions: Conceptualization, A.S.E.-S. and A.A.S.; methodology, A.S.E.-S. and A.A.S.; software, A.S.E.-S. and A.A.S.; validation, A.S.E.-S. and A.A.S.; data curation, A.A.S.; writing—original draft preparation, A.S.E.-S. and A.A.S.; writing—review and editing, A.S.E.-S. and A.A.S.; supervision, A.S.E.-S.; project administration, A.S.E.-S. All authors have read and agreed to the published version of the manuscript.

Funding: This research was funded by Ongoing Research Funding program (ORF-2026-1044), King Saud University, Riyadh, Saudi Arabia.

Data Availability Statement: All data generated or analyzed during this study are included in this published article and its Supplementary Materials.

Conflicts of Interest: The authors declare no conflicts of interest.

References

1. Hou, D.; Jia, X.; Wang, L.; McGrath, S.P.; Zhu, Y.G.; Hu, Q.; Zhao, F.J.; Bank, M.S.; O'Connor, D.; Nriagu, J. Global soil pollution by toxic metals threatens agriculture and human health. *Science* **2025**, *388*, 316–321. [CrossRef] [PubMed]
2. Tóth, G.; Hermann, T.; Da Silva, M.R.; Montanarella, L. Heavy metals in agricultural soils of the European Union with implications for food safety. *Environ. Int.* **2016**, *88*, 299–309. [CrossRef] [PubMed]
3. Neal, A.P.; Guilarte, T.R. Mechanisms of lead and manganese neurotoxicity. *Toxicol. Res.* **2013**, *2*, 99–114. [CrossRef] [PubMed]
4. Häder, D.P.; Helbling, E.W.; Villafañe, V.E. *Anthropogenic Pollution of Aquatic Ecosystems*; Springer Nature: Cham, Switzerland, 2021; Volume 426. [CrossRef]
5. Khaleeq, A.; Ahmed, M.; Huma, R.; Mujtaba, A.; Noor, S.; Rehman, R.; Sheikh, T.A.; Qamar, S.; Iqbal, D.N.; Alharthy, R.D.; et al. Evaluation of trace and heavy metals in different varieties of sauces to characterize their impact on human health. *J. Food Compos. Anal.* **2022**, *114*, 104789. [CrossRef]
6. Song, Q.; Li, J. A review on human health consequences of metals exposure to e-waste in China. *Environ. Pollut.* **2015**, *196*, 450–461. [CrossRef] [PubMed]
7. Pan, L.; Wang, Y.; Ma, J.; Hu, Y.; Su, B.; Fang, G.; Wang, L.; Xiang, B. A review of heavy metal pollution levels and health risk assessment of urban soils in Chinese cities. *Environ. Sci. Pollut. Res.* **2017**, *25*, 1055–1069. [CrossRef] [PubMed]
8. El-Sorogy, A.S.; Al Khathlan, M.H. Assessment of potentially toxic elements and health risks of agricultural soil in Southwest Riyadh, Saudi Arabia. *Open Chem.* **2024**, *22*, 20240017. [CrossRef]
9. Jiang, Y.; Guo, H.; Chen, K.; Fei, X.; Li, M.; Ma, J.; He, W. Health risk assessment for potential toxic elements in the soil and rice of typical paddy fields in Henan Province. *Toxics* **2024**, *12*, 771. [CrossRef] [PubMed]
10. Orosun, M.M.; Nwabachili, S.; Alshehri, R.F.; Omeje, M.; Alshdoukhi, I.F.; Okoro, H.K.; Ogunkunle, C.O.; Louis, H.; Abdulhamid, F.A.; Osahon, S.E.; et al. Potentially toxic metals in irrigation water, soil, and vegetables and their health risks using Monte Carlo models. *Sci. Rep.* **2023**, *13*, 21220. [CrossRef] [PubMed]
11. De Miguel, E.; Iribarren, I.; Chacón, E.; Ordoñez, A.; Charlesworth, S. Risk-based evaluation of the exposure of children to trace elements in playgrounds in Madrid, Spain. *Chemosphere* **2007**, *66*, 505–513. [CrossRef] [PubMed]
12. Rahman, M.S.; Kumar, P.; Ullah, M.; Jolly, Y.N.; Akhter, S.; Kabir, J.; Begum, B.A.; Salam, A. Elemental analysis in surface soil and dust of roadside academic institutions in Dhaka city, Bangladesh and their impact on human health. *Environ. Chem. Ecotoxicol.* **2021**, *3*, 197–208. [CrossRef]

13. Agyeman, P.C.; John, K.; Kebonye, N.M.; Borůvka, L.; Vašát, R.; Drábek, O.; Němeček, K. Human health risk exposure and ecological risk assessment of potentially toxic element pollution in agricultural soils in the district of Frydek Mistek, Czech Republic: A sample location approach. *Environ. Sci. Eur.* **2021**, *33*, 137. [CrossRef]
14. Gong, C.; Wang, S.; Wang, D.; Lu, H.; Dong, H.; Liu, J.; Yan, B.; Wang, L. Ecological and human health risk assessment of heavy metal(loid)s in agricultural soil in hotbed chives hometown of Tangchang, Southwest China. *Sci. Rep.* **2022**, *12*, 8563. [CrossRef] [PubMed]
15. Kristamtini; Widyayanti, S.; Widodo, S.; Pustika, A.B.; Purwaningsih, H.; Hanifa, A.P.; Muazam, A.; Sutardi; Badia Ginting, R.C.; Mulia, S.; et al. Potentially toxic elements' spatial distribution in agricultural soils and their impact on ecological and health risks. *Case Stud. Chem. Environ. Eng.* **2024**, *10*, 100936. [CrossRef]
16. Wu, Y.; Xia, Y.; Mu, L.; Liu, W.; Wang, Q.; Su, T.; Yang, Q.; Milinga, A.; Zhang, Y. Health risk assessment of heavy metals in agricultural soils based on multi-receptor modeling combined with Monte Carlo simulation. *Toxics* **2024**, *12*, 643. [CrossRef] [PubMed]
17. Sultana, A.; Wang, Q.; Suzuki, M.; Enyoh, C.E.; Rana, M.S.; Isobe, Y.; Wang, W. Heavy metal contamination in homestead agricultural soils of bangladesh: Industrial influence, human exposure and ecological risk assessment. *Soil Syst.* **2025**, *9*, 136. [CrossRef]
18. El-Sorogy, A.S.; Alharbi, T.; Almadani, S.A.; Shoaib, S.; Rikan, N.; Meroño de Larriva, J.E.; Shokr, M.S. An integrated GIS–statistical approach to assess soil contamination in Al-Muzahmiya, Saudi Arabia: Implications for food security. *Front. Sustain. Food Syst.* **2025**, *9*, 1695962. [CrossRef]
19. Al-Hashim, M.H.; El-Sorogy, A.S.; Alhejji, S.S.; Rikan, N. Assessing potentially toxic element contamination in agricultural soils of an arid region: A multivariate and geospatial approach. *Minerals* **2026**, *16*, 93. [CrossRef]
20. Alarifi, S.S.; El-Sorogy, A.S.; Al-Kahtany, K.; Alharbi, T.; Alhejji, S.S.S.; de Larriva, J.E.M.; Shokr, M.S. Exploring soil heavy metal(loid) levels in Huraymla, Saudi Arabia: Implications for sustainable agriculture and food supply. *Front. Sustain. Food Syst.* **2026**, *9*, 1726872. [CrossRef]
21. Li, W.; Cao, X.; Hu, Y.; Cheng, H. Source Apportionment and Risk Assessment of Heavy Metals in Agricultural Soils in a Typical Mining and Smelting Industrial Area. *Sustainability* **2024**, *16*, 1673. [CrossRef]
22. Tong, L.; Yang, A.; Fan, M.; Zheng, D.; Li, J.; Liu, H.; Li, C.; Tang, Y.; Cheng, L. Assessment of Heavy Metal Sources and Health Risks in Soil-Crop Systems of Fragmented Farmland. *Front. Public Health* **2025**, *13*, 1637595. [CrossRef] [PubMed]
23. Fan, W.; Zhou, J.; Zheng, J.; Wang, S.; Du, J.; Hu, L.; Shan, R.; Zhang, L. Quantitative Source Apportionment and Source-Oriented Health Risk of Heavy Metals in Soils: A Case Study of Yutian County in the Southern Margin of Tarim Basin, China. *Agronomy* **2025**, *15*, 2721. [CrossRef]
24. ALS Arabia. *QC Certificate of Analysis JD26028672*; Australian Laboratory Services Arabia Co. Ltd.: Jeddah, Saudi Arabia, 2026.
25. Tomlinson, D.L.; Wilson, J.G.; Harris, C.R.; Jeffrey, D.W. Problems in the assessment of heavy-metal levels in estuaries and the formation of a pollution index. *Helgol. Meeresunters.* **1980**, *33*, 566–575. [CrossRef]
26. Nemerow, N.L. *Stream, Lake, Estuary, and Ocean Pollution*, 2nd ed.; Van Nostrand Reinhold: New York, NY, USA, 1991.
27. Wen, Y.; Wang, Y.; Ji, W.; Wu, S.; Gong, Y.; Meng, X. Pollution Levels and Associated Health Risks of Heavy Metals in Agricultural Soils in Zhenjiang and Yangzhou, China. *Agriculture* **2025**, *15*, 2552. [CrossRef]
28. Alsafran, M.; Usman, K.; Al Jabri, H.; Rizwan, M. Ecological and health risks assessment of potentially toxic metals and metalloids contaminants: A case study of agricultural soils in Qatar. *Toxics* **2021**, *9*, 35. [CrossRef] [PubMed]
29. U.S. EPA. *Regional Screening Levels (RSLs): User's Guide*; U.S. Environmental Protection Agency: Washington, DC, USA, 2025.
30. Xu, S.; Yu, C.; Wang, Q.; Liao, J.; Liu, C.; Huang, L.; Liu, Q.; Wen, Z.; Feng, Y. Chromium contamination and health risk assessment of soil and agricultural products in a rural area in southern China. *Toxics* **2022**, *11*, 27. [CrossRef] [PubMed]
31. U.S. EPA. *Exposure Factors Handbook: 2011 Edition*; EPA/600/R-09/052F; U.S. Environmental Protection Agency: Washington, DC, USA, 2011.
32. U.S. EPA. *Update for Chapter 5 of the Exposure Factors Handbook: Soil and Dust Ingestion*; EPA/600/R-17/384F; U.S. Environmental Protection Agency: Washington, DC, USA, 2017.
33. U.S. EPA. *Supplemental Guidance for Developing Soil Screening Levels for Superfund Sites*; Office of Emergency and Remedial Response, U.S. Environmental Protection Agency: Washington, DC, USA, 2002.
34. Miletic, A.; Lucic, M.; Onjia, A. Exposure factors in health risk assessment of heavy metal(loid)s in soil and sediment. *Metals* **2023**, *13*, 1266. [CrossRef]
35. Alharbi, T.; Nour, H.E.; Al-Kahtany, K.; Zumlot, T.; El-Sorogy, A.S. Health risk assessment and contamination of lead and cadmium levels in sediments of the northwestern Arabian Gulf coast. *Heliyon* **2024**, *10*, e36447. [CrossRef] [PubMed]
36. Alharbi, T.; El-Sorogy, A.S. Spatial distribution and risk assessment of heavy metals pollution in soils of marine origin in central Saudi Arabia. *Mar. Pollut. Bull.* **2021**, *170*, 112605. [CrossRef] [PubMed]
37. Wang, L.; Liu, Q.; Bai, R. Soil heavy metal pollution and health risk assessment based on Monte Carlo simulation: Case study of Xicheng Lead-Zinc Mining Area. *Sustainability* **2025**, *17*, 3963. [CrossRef]

38. Xia, F.; Zhao, Z.; Niu, X.; Wang, Z. Integrated pollution analysis, pollution area identification and source apportionment of heavy metal contamination in agricultural soil. *J. Hazard. Mater.* **2024**, *465*, 133215. [CrossRef] [PubMed]
39. Liu, Z.; Wang, L.; Yan, M.; Tian, Y.; Ma, B.; Xie, Q. Heavy metal synergistic pollution risk assessment in the soil-crop system of the Nanyang Basin. *Sci. Rep.* **2025**, *15*, 19937. [CrossRef] [PubMed]
40. Qu, C.S.; Ma, Z.W.; Yang, J.; Liu, Y.; Bi, J.; Huang, L. Human exposure pathways of heavy metals in a lead-zinc mining area, Jiangsu Province, China. *PLoS ONE* **2012**, *7*, e46793. [CrossRef] [PubMed]
41. Bello, S.; Nasiru, R.; Garba, N.N.; Adeyemo, D.J. Carcinogenic and noncarcinogenic health risk assessment of heavy metals exposure from Shanono and Bagwai artisanal gold mines, Kano State, Nigeria. *Sci. Afr.* **2019**, *6*, e00197. [CrossRef]
42. Bello, O.S.; Abdulsalam, I.O.; Sridhar, M.K.C.; Taiwo, A.M. Human health risk assessment via the dietary intake of heavy metal(loid)s from the consumption of vegetables grown in soils from Katsina State, Nigeria. *Hum. Ecol. Risk Assess. Int. J.* **2019**, *25*, 2162–2180.
43. Mondal, P.; Lofrano, G.; Carotenuto, M.; Guida, M.; Trifuoggi, M.; Libralato, G.; Sarkar, S.K. Health risk and geochemical assessment of trace elements in surface sediment along the Hooghly (Ganges) River Estuary, India. *Water* **2021**, *13*, 110. [CrossRef]
44. Siddig, M.M.S.; Brevik, E.C.; Sauer, D. Human health risk assessment from potentially toxic elements in the soils of Sudan: A meta-analysis. *Sci. Total Environ.* **2025**, *958*, 178196. [CrossRef] [PubMed]
45. Leng, Q.; Ren, D.; Wang, Z.; Zhang, S.; Zhang, X.; Chen, W. Assessment of potentially toxic elements pollution and human health risks in polluted farmland soils around distinct mining areas in China—A case study of Chengchao and Tonglushan. *Toxics* **2023**, *11*, 574. [CrossRef] [PubMed]
46. Tian, S.; Wang, S.; Bai, X.; Zhou, D.; Luo, G.; Yang, Y.; Hu, Z.; Li, C.; Deng, Y.; Lu, Q. Ecological security and health risk assessment of soil heavy metals on a village-level scale, based on different land use types. *Environ. Geochem. Health* **2020**, *42*, 3393–3413. [CrossRef] [PubMed]
47. Ahmad, W.; Zubair, M.; Ahmed, M.; Ahmad, M.; Latif, S.; Hameed, A.; Kanwal, Q.; Iqbal, D.N. Assessment of potentially toxic metal(loid)s contamination in soil near the industrial landfill and impact on human health: An evaluation of risk. *Environ. Geochem. Health* **2023**, *45*, 4353–4369. [CrossRef] [PubMed]
48. Al-Kahtany, K.; El-Sorogy, A.S. Contamination and health risk assessment of surface sediments along Ras Abu Ali Island, Saudi Arabia. *J. King Saud Univ. Sci.* **2023**, *35*, 102509. [CrossRef]
49. Varol, M.; Gündüz, K.; Sünbül, M.R. Pollution status, potential sources and health risk assessment of arsenic and trace metals in agricultural soils: A case study in Malatya province, Turkey. *Environ. Res.* **2021**, *202*, 111806. [CrossRef] [PubMed]
50. Alarifi, S.S.; El-Sorogy, A.S.; Al-Kahtany, K.; Hazaea, S.A. Contamination and health risk assessment of potentially toxic elements in Al-Ammariah agricultural soil, Saudi Arabia. *J. King Saud Univ. Sci.* **2023**, *35*, 102826. [CrossRef]
51. Gevorgyan, G.A.; Ghazaryan, K.A.; Movsesyan, H.S.; Zhamharyan, H.G. Human health risk assessment of heavy metal pollution in soils around Kapan mining area, Armenia. *Electron. J. Nat. Sci.* **2017**, *2*, 29–33.
52. Yang, B.; Li, W.; Xiong, J.; Yang, J.; Huang, R.; Xie, P. Health risk assessment of heavy metals in soil of Lalu Wetland based on Monte Carlo simulation and ACPS-MLR. *Water* **2023**, *15*, 4223. [CrossRef]
53. Zhang, J.; Li, H.; Zhou, Y.; Dou, L.; Cai, L.; Mo, L.; You, J. Bioavailability and soil-to-crop transfer of heavy metals in farmland soils: A case study in the Pearl River Delta, South China. *Environ. Pollut.* **2018**, *235*, 710–719. [CrossRef] [PubMed]
54. Luo, H.; Wang, P.; Wang, Q.; Lyu, X.; Zhang, E.; Yang, X.; Han, G.; Zang, L. Pollution sources and risk assessment of potentially toxic elements in soils of multiple land use types in the arid zone of Northwest China based on Monte Carlo simulation. *Ecotoxicol. Environ. Saf.* **2024**, *279*, 116479. [CrossRef] [PubMed]

Disclaimer/Publisher's Note: The statements, opinions and data contained in all publications are solely those of the individual author(s) and contributor(s) and not of MDPI and/or the editor(s). MDPI and/or the editor(s) disclaim responsibility for any injury to people or property resulting from any ideas, methods, instructions or products referred to in the content.